The effect of silica and carbon as modified of calcium-alginate membrane for desalination

Anugrah Ricky Wijaya[1*], *Alif Alfarisyi* Syah[1], *Chandra Kusuma* Wardani[1], and *Nisrina Safa* Kamila[1]

[1]Departement of Chemistry, Faculty of Mathematic and Natural Science, Universitas Negeri Malang, 65145 Jl. Semarang 5 Malang, Malang, Indonesia

Abstract. In order to improve the performance of the calcium alginate membrane, we modified it to add the silica and carbon as the potential to absorb NaCl as the desalination materials. The novelty of this study, the natural resources of coral skeletons, beach sand, and the mangrove leaves were utilized as the source of Ca, Si and C for membrane fabrication, respectively. The results indicate the calcium alginate-carbon membrane with its mangrove leaves as the activated carbon proved effective to reduce salt levels. FTIR analysis of this membrane revealed the presence of functional groups like -OH, C=O, and C-O as the evidence to absorb NaCl. The SEM analysis displayed a rugged membrane surface with an average particle diameter of 347.98 nm. This membrane was capable of adsorbing approximately 49.05%/20-minutes and 46.7%/30-minutes of Na^+ and Cl^- ions with 0.05 grams of activated carbon, respectively. The calcium alginate-silica analysis also indicated the presence of functional groups (-OH, C=O, C-O, Si-O, and Si-OH) facilitating the NaCl binding process. Additionally, SEM analysis depicted a porous structural morphology with a particle size diameter of approximately 16192.78 nm. This membrane was capable of adsorbing approximately 55.04%/20-minutes and 49.4%/40-minutes of Na^+ and Cl^- ions with 0.05 grams of activated carbon, respectively. The comparison between the two membranes revealed significant differences in their NaCl ion absorption capacities. The calcium alginate-silica membrane tended to exhibit slightly higher absorption capacity compared to the calcium alginate-carbon membrane under the specified optimal conditions.

1 Introduction

Water scarcity in the coastal areas poses important challenges in securing clean water sources that are important for the survival of life. With 3% of the earth's water being fresh water and increasing pollution of coastal well water by sea water, the need for innovative water purification methods is urgent [1]. Some researchers protected the environment using the surface water, sea water, sediment as the media to detect the source of metal contents and natural sources. The natural sources especially in the estuary of seawater can be treated as

* Corresponding author: anugrah.ricky.fmipa@um.ac.id

clean water with low salinity. The permissible threshold for clean water salinity is ≤ 0.05 ppt, some exceeded place was found in the coastal areas, including the Gulf of Prigi [2–4].

Desalination is an important technique for reducing the high salinity levels, which the dominant salt components, Na^+ and Cl^- ions [5]. Researcher have studied the analysis of minerals distribution and determination methods in seawater [6–7]. The adsorption technology with a low energy consumption method is emerging as a promising solution and involves membrane-based separation of Na^+ and Cl^- ions. Some natural sources like coral skeletons and beach sand that are abundantly surrounding seawater can be applied to be material of desalination. Coral skeletons have a high calcium content, important for adsorption due to their porous structure. The transformation of this framework into calcium carbonate ($CaCO_3$) serves as a valuable resource for the adsorption process [8]. Calcium ions from the coral skeleton cross-link with sodium alginate is predicted to form alginate and strengthen its structure. The incorporating activated carbon into the calcium alginate membrane is considered for increasing its adsorption capacity. The activated carbon has porous nature and effective adsorption properties, complements polymer membranes by providing additional active sites for ion binding. Although previous research has shown the potential of activated carbon in reducing seawater salinity, limitations in its adsorption capacity still exist [9].

The one material is suspected as the advanced material is alginate. Alginate, a gelling agent rich in active functional groups (-COO^- and -OH^-) forms a gel when combined with divalent Ca^{2+} ions to intensify the gelation process. The addition of silica to Ca-alginate-silica increases the adsorption capacity of alginate due to the content silica, which has siloxane (Si-O-Si) and silanol (Si-OH) groups. It is suited to improve the performance of the adsorption properties towards polar molecules such as NaCl. In this study, we applied the silica from beach sand which was characterized by crystalline silica (SiO_2) and removed the impurity compounds to increase the membrane expansion capacity. Besides silica, the activated carbon could be applied to Ca-alginate membranes for improving the adsorption capacity [10]. The high adsorption capacity of activated carbon-alginate adsorbent for heavy metal adsorption has been well documented. Cazetta, et all (2011) reported the activated carbon from mangrove roots with NaOH activation showed high surface area and pore development[11].

Here, we used the membrane synthesis using natural waste materials, such as the coral skeletons, mangrove leaves, and beach sand as the Ca, C, and SiO_2, respectively. It offers to improve the performance of membranes modified with natural sources to provide clean water. In addition, the comparative study of calcium alginate silica and carbon membranes aims to evaluate the efficiency of each in reducing salt contents in perspective to reduce NaCl levels. Furthermore, this study is expected not only as a laboratory-scale exploration continuing its application of membranes for large-scale seawater desalination.

2 Material and Method

2.1 Preparation of 0.5 M $CaCl_2$ Solution of Coral Skeleton

The coral was washed using distilled water while brushing and dried at 60 ^oC. The coral was then ground and sieved with a size of 200 mesh. The powder that passed the sieve was calcined at 800 ^oC for 2 hours to produce $CaCO_3$. $CaCl_2$ solution was made from 5 grams of calcined coral added to 100 mL of 1M HCl solution. The solution was then stirred until homogeneous at 35 ^oC for 60 minutes. The mixture was filtered and the resulting filtrate was a 0.5 M $CaCl_2$ solution.

2.2 Preparation and Extraction of Silica (SiO_2) from Beach Sand

Beach sand was dried at 60 ºC for 4 days. The dried sand sample was pulverized and sieved with a size of 100 mesh. The sieved sample was cleaned again using a magnet to separate the iron impurities attached to the sand. The 120 grams sample was added 50 mL of hot distilled water, 150 mL of 37% w/v HCl, and 50 mL of 65% w/v HNO_3, allowed to stand for 20 hours in a fume hood. The mixture sample was then deconstructed using reflux at ±70 ºC for 2 hours, and cooled at room temperature. The sample was then filtered and neutralized to pH 7. The residue was then dried at 60 ºC for 1 hour.

The residue sample was then calcined using a furnace at 600 ºC for 4 hours to become sand ash. The calcined sand sample was added 30 mL of hot distilled water and 30 mL of concentrated HCl and then evaporated 3 times to dry. The sample was added 30 mL of concentrated HCl solution and heated at 60 ºC for 35 minutes. The sample was neutralized with distilled water and the residue was obtained. The residue was calcined at 600 ºC for 4 hours and obtained 40 grams of white silica powder.

2.3 The Synthesis of Activated Carbon from Mangrove Leaves

The cleaned mangrove leaves were dried at 60 °C until dryness. The dried sample was then pulverized and sieved to obtain a 200-mesh size powder. The powder sample was carbonized using a furnace at 400 °C for 2 hours. The sample was chemically activated using 0.5 M KOH (potassium hydroxide), soaked in 0.5 M KOH for 24 hours, filtered and washed with distilled water until a neutral pH. After neutralization, the carbon sample was finally dried at 60 °C.

2.4 Fabrication of Ca-Alginate-Silica Membrane

Optimization was carried out with silica mass variations of 0, 0.025, 0.05, and 0.075g silica and alginate concentration variations of 0.5, 1, and 2% w/v. The mixture was then poured into a mold and added of 0.5 M $CaCl_2$ solution. It was allowed to stand for 18 hours and the molded membrane was lifted in the form of a transparent box and solid texture. The membrane was washed 8 times using 100 mL of distilled water for 15 minutes per wash. The each silica mass variation was stirred using a waterbath shaker for 40 minutes at 130 rpm. After stirring, the filtrate was analyzed for Cl^- ion content using argentometric titration in duplicate.

2.5 Fabrication of Ca-Alginate-C Membrane

Two different alginate concentrations, 1% and 2% w/v, were utilized. After homogenization, 25 mL of 1% alginate solution was taken and mixed with 0.05 gram of activated carbon to produce the 1% alginate-carbon membrane. In case of the 2% alginate concentration, 25 mL of 2% alginate solution was mixed with 0.05 gram of activated carbon to create the 2% alginate-carbon membrane. That membranes with varying alginate concentrations play a crucial role in the subsequent phases of our research.

To produce the alginate-carbon membranes after optimizing concentration alginate (1% w/v), we initially added 25 mL of this alginate solution with varied masses 0, 0.05, 0.075, and 0.1 gram of activated carbon, respectively. The mixture sample was then stirred until a consistent blend. This process was undertaken with the aim of optimizing the quantity of activated carbon within the alginate-carbon membrane for the most efficient adsorption performance. The mixture of alginate and carbon was stirred until blending. This alginate-carbon mixture was then poured into a petri dish. Subsequently, 10 mL of $CaCl_2$ solution was

slowly added to the alginate-carbon mixture and left to stand for 24 hours. The alginate-carbon membrane was created and washed with distilled water until no contained chloride ions using tested $AgNO_3$.

The optimum Ca-alginate-carbon membrane was characterized using FTIR for functional group analysis and SEM to determine surface morphology. Co and Ce (mg/L) indicate the concentration of NaCl before and after the adsorption process.

3 Results and Discussion

3.1 Preparation of $CaCO_3$ from Coral Skeleton

Coral skeleton sample was subjected to XRF characterization to determine the composition of its compounds, before and after calcination. The characterization results are listed in Tables 1 and 2.

Table 1. Composition of coral before calcination

Coral			
Element	**Wt (%)**	**Oxide**	**Wt (%)**
Si	1.30	SiO_2	2.30
Ca	90.82	CaO	90.86
Ti	0.15	TiO_2	0.16
Mn	0.073	MnO	0.063
Fe	1.70	CuO	0.028
Cu	0.034	SrO	3.42
Sr	4.40	MoO_3	1.1
Mo	0.89	BaO	0.10
Ba	0.1	Yb_2O_3	0.35
Yb	0.47	Lu_2O_3	0.06
Lu	0.09		

Table 2. Composition of coral after calcination

Coral			
Element	**Wt (%)**	**Oxide**	**W (%)**
Ca	92.58	CaO	93.41
Ti	0.11	TiO_2	0.12
Mn	0.06	MnO	0.052
Fe	1.49	Fe_2O_3	1.43
Cu	0.04	CuO	0.034
Sr	4.54	SrO	3.56
Mo	1.1	MoO_3	1.3
Ba	0.1	BaO	0.08

Based on the XRF test results, the CaO content in the coral skeleton from Prigi Beach before and after calcination amounted to 90.8% and 93.41%. The high content of CaO in coral has great potential as an adsorbent constituent to increase the strength of the gel in the membrane.

3.2 Fourier Transform Infrared Spectroscopy (FTIR) Characterization of Coral Skeleton

As shown in Fig. 1, the FTIR spectrum contained in the coral after calcination at 800°C. The IR spectra showed the appearance of absorption at wave number 713.66 cm^{-1} indicating the

presence of Ca-O group. At wave numbers 873.75 - 1797.65 cm^{-1}, it reflects the C-O group which is a common characteristic of carbonate ions in calcium carbonate.

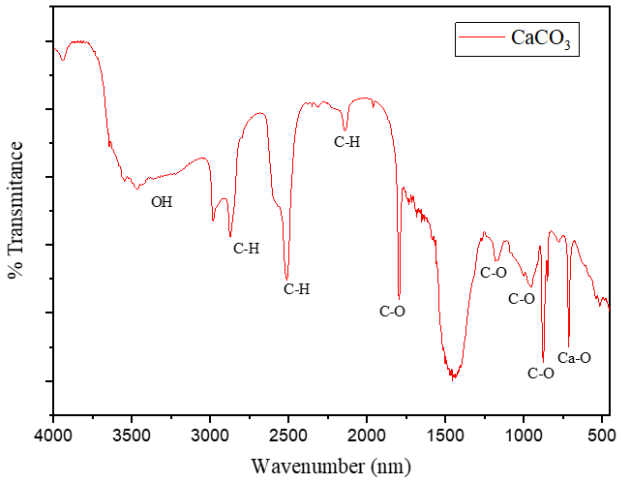

Fig. 1. FTIR spectra of calcined coral at 800 °C

Other absorption also appeared at wave numbers 2139.05, 2513.24, and 2873.93 cm^{-1} which is the vibration of the C-H group. The non-wide FTIR spectrum shows that there unknown source in the calcined $CaCO_3$ reflecting a natural material from coral skeletons mixed with impurities [12].

3.3 Preparation and Extraction of Silica from Beach Sand

As shown in Table 3, the preparation of Si was carried out by soaking 120 grams of beach sand with a mixture of 150 mL of 37% HCl and 50 mL of 69% HNO_3 for 20 hours to remove metal oxide impurities. Silica extraction was carried out by means of closed wet deconstruction of the mixture using aqua regia solvent with reflux at ±70 °C for 2 hours. Silica extraction produced 40 grams of white powder and continued with XRF and FTIR characterization.

Table 3. Composition of beach sand before extraction

Beach Sand			
Unsur	**Wt (%)**	**Oksida**	**Wt (%)**
Si	10.0	SiO_2	16.2
S	0.24	SO_3	0.81
K	0.1	K_2O	0.01
Ca	44.6	CaO	42.2
Ti	4.23	TiO_2	4.64
V	0.30	V_2O_5	0.25
Cr	0.085	Cr_2O_3	0.086
Mn	0.44	MnO	0.34
Fe	36.4	Fe_2O_3	32.1
Cu	0.065	CuO	0.049
Sr	2.3	SrO	1.6
Zr	0.10	In_2O_3	1.0
In	0.4	Eu_2O_3	0.3
Eu	0.3	HgO	0.35
Hg	0.49		

Table 4. Composition of beach sand after extraction

Beach Sand			
Unsur	**Wt (%)**	**Oksida**	**Wt (%)**
Si	78.5	SiO_2	89.5
K	1.4	K_2O	0.61
Ca	9.00	CaO	4.55
Ti	3.27	TiO_2	1.86
V	0.090	V_2O_5	0.02
Mn	0.24	MnO	0.092
Fe	6.87	Fe_2O_3	3.09
Cu	0.095	CuO	0.035
Sr	0.45	SrO	0.16
Eu	0.1	Eu_2O_3	0.08

As shown in Table 4, the XRF test results show that the SiO_2 content in Prigi Bay beach sand before and after extraction amounted to 16.2% and 89.5% wt, respectively. The increase in SiO_2 content was followed by a change in color from brownish to white after synthesis.

As shown in Fig. 2, the FTIR results on beach sand after silica extraction, it shows the presence of extended stretching vibrations of the -OH functional group, silanol (Si-OH) at wave number 3365.78 cm^{-1}. The presence of the -OH group is reinforced by the appearance of absorption at wave number 1612.49 cm^{-1} which is the bending vibration of the -OH group of the Si-OH bond.

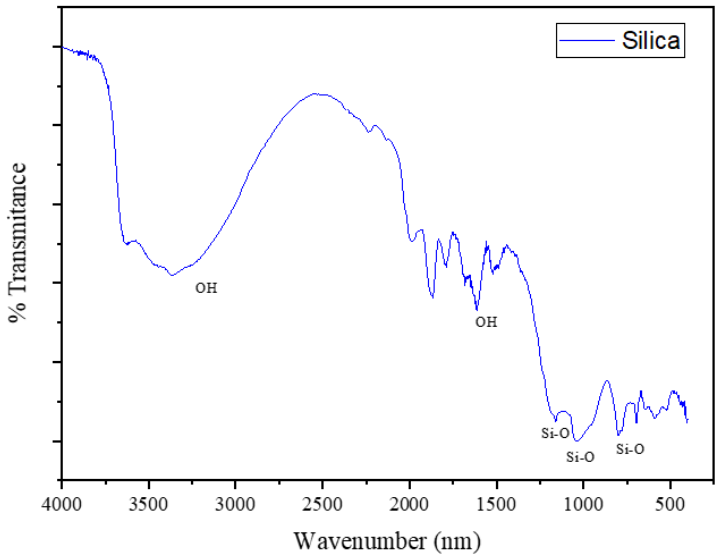

Fig. 2. FTIR spectrum of silica extraction from beach sand

Other absorption also appeared at wave numbers 804.31, 1159.5, and 1045.41 cm^{-1} which are bending vibrations, asymmetric stretching vibrations, and stretching vibrations of Si-O groups from siloxane groups (Si-O-Si), respectively. The silica from beach sand contains silanol and siloxane groups with wave numbers 3380 cm^{-1} and 935.47 cm^{-1} which are vibrations of the -OH group of Si-OH and vibrations of the Si-O-Si bond in SiO_2.

3.4 Preparation and extraction of Activated Carbon from Mangrove Leaf

The synthesized activated carbon was analyzed using XRF to determine the elements and metal oxides present within it. The components of the activated carbon is listed in Table 5.

Table 5. XRF analysis of Activated Carbon

Elements	Wt (%)	Elements	Wt (%)	Elements	Wt (%)
Si	1.1	Sr	2.1	SiO_2	1.9
P	1.0	Eu	0.2	P_2O_5	1.9
S	1.2	Yb	0.5	CaO	80.4
K	0.4	Re	0.7	TiO_2	0.33
Ca	81.3	SO_3	2.5	NiO	0.1
Ti	0.30	K_2O	0.38	ZnO	0.2
Mn	4.63	MnO	3.97	SrO	1.6
Fe	5.78	Fe_2O_3	5.37	Yb_2O_3	0.4
Cu	0.46	CuO	0.37		
Zn	0.2	Re_2O_7	0.70		

The characterization of activated carbon using XRF aimed to determine the components present in the activated carbon before its use in membrane production. The elements found in activated carbon can influence its adsorption capacity, potentially affecting ion uptake. Based on the XRF results, the activated carbon contains various impurities. The highest impurities are calcium (Ca) and iron (Fe). These impurities can obstruct pores and impact pore size [13].

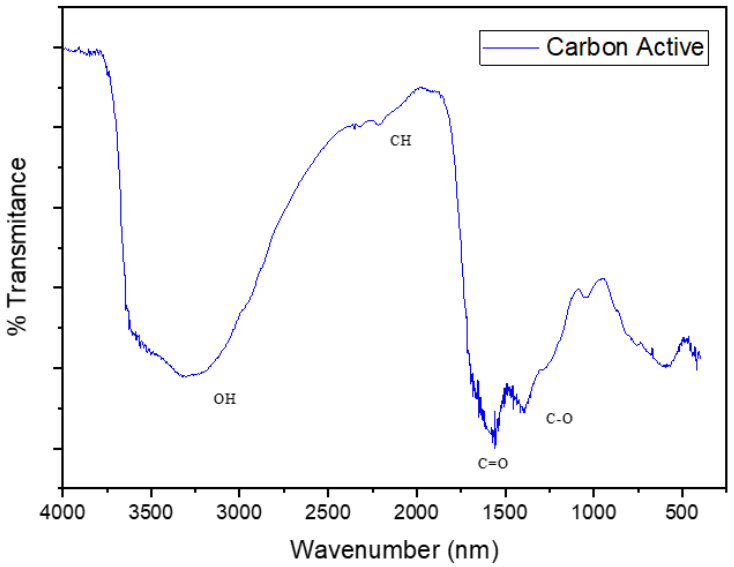

Fig. 3. FTIR spectrum of carbon extraction from mangrove leaves

As shown in Fig. 3, the FT-IR spectrum of mangrove leaf activated carbon exhibits absorption peaks in the region of 3253.91 cm^{-1}, indicating the presence of hydroxyl (-OH) groups. In the absorption region at 1585.48 cm^{-1}, carbonyl (C=O) groups are observed. The absorption band at 1259.52 cm^{-1} indicates the presence of carboxyl (C–O) groups.

3.5 Characterization of the Ca-Alginate-Carbon and Ca-Alginate-Silica Membrane Using FTIR

IR analysis was performed to identify functional groups present in silica from beach sand, mangrove leaf activated carbon, Ca-alginate, Ca-alginate-silica and Ca-alginate carbon membrane. This comparison aimed to determine the influence of adding silica and activated carbon to the Ca-alginate membrane. The FTIR results for the Ca-alginate-carbon membrane, Ca-alginate-silika, Ca-alginate, silica and mangrove leaf activated carbon are presented in Fig. 4.

The FT-IR spectrum of the Ca-alginate membrane reveals an absorption band at 3647.39 cm^{-1}, indicating the presence of O–H groups. The absorption bands at 2943.37 cm^{-1} correspond to C-H groups, while the band at 1674.21 cm^{-1} signifies the existence of C=O groups. Additionally, the bands at 1450.46 cm^{-1} and 1192.00 cm^{-1} are associated with C–O groups. In the FT-IR spectrum of the Ca-alginate-carbon membrane, the absorption band at 3302.13 cm^{-1} is attributed to O–H groups (hydroxyl). The band at 2927.94 cm^{-1} corresponds to C–H vibrations, while the peak at 1598.98 cm^{-1} indicates C=O bonds. Furthermore, the bands at 1423.46 cm^{-1} and 1035.77 cm^{-1} suggest the presence of C–O groups.

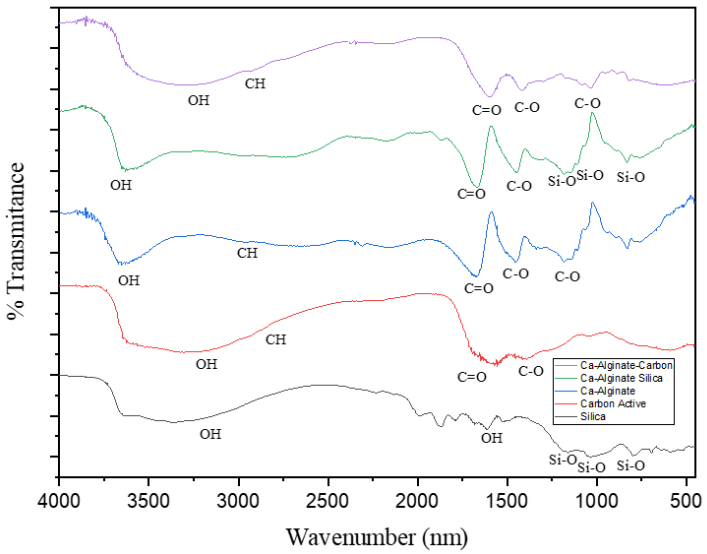

Fig. 4. spectra IR of silica, carbon, ca-alginate membrane, ca-alginate-silica, and ca-alginate-carbon.

The FTIR spectrum results for the Ca-alginate-carbon membrane show a peak at 3302.13 cm^{-1}, signifying the vibration of -OH groups from hydroxyl groups. The hydroxyl peak in Ca-alginate membrane without activated carbon addition was observed at 3647.39 cm^{-1}, and in Ca-alginate-carbon membrane, the O–H group showed a broad peak at 3296.48 cm^{-1}. This suggests that the Ca-alginate-carbon membrane has O–H groups bonded to the activated carbon's hydroxyl groups. The -OH groups experience a widening of the band when activated carbon is added to the Ca-alginate membrane. Both Ca-alginate and Ca-alginate-carbon membranes exhibit characteristic fingerprint regions for guluronate in the absorption range of 900-890 cm^{-1} and mannonate in the absorption range of 850-810 cm^{-1}.

The results of FTIR analysis on Ca-alginate-silica showed a shift in the wave number of the stretching vibration of the -OH group at 3630.03 cm^{-1}. Other absorbances also appear at wave numbers 1668.42 cm^{-1} and 1110.9 cm^{-1} which are vibrations of the C=O group and the C-O group of guluronic acid in alginate. Moreover, the peak at wave number 1591 cm^{-1}

indicates the presence of carbonyl bond stretching vibrations (C=O) from carboxylic groups. When compared to Ca-alginate, there is a shift in the wave number of the -OH group which has shifted the wave number from 3653.17 cm^{-1} in Ca-alginate to 3630.03 cm^{-1}. This is assumed to be the presence of hydrogen bonds from silanol groups (Si-OH) resulting in widened peaks and shifting the absorption band to the right, to lower wave numbers, indicating the energy is getting smaller. The wave number 1668.42 cm^{-1} also shows a shift in the carbonyl group (C=O) in calcium alginate silica and the wave number 1107.14 cm^{-1} indicates the stretching of the C-O bond in the C-O-C structure of guluronic and mannuronic acids.

3.6 Characterization of the Ca-Alginate-Carbon and Ca-Alginate- Silica Membrane Using SEM

3.6.1 Characterization of the Ca-Alginate-Silica Membrane Using SEM

SEM characterization of the membrane was carried out to determine the microstructure and surface morphology of the membrane at the most optimum composition for the seawater absorption process. In analyzing the membrane pore morphology from the SEM instrument, it was carried out using ImageJ and OriginLab 2023 software to determine the particle size distribution. The results obtained a particle size diameter of 16192.78 nm with a porous structure morphology and relatively rough.

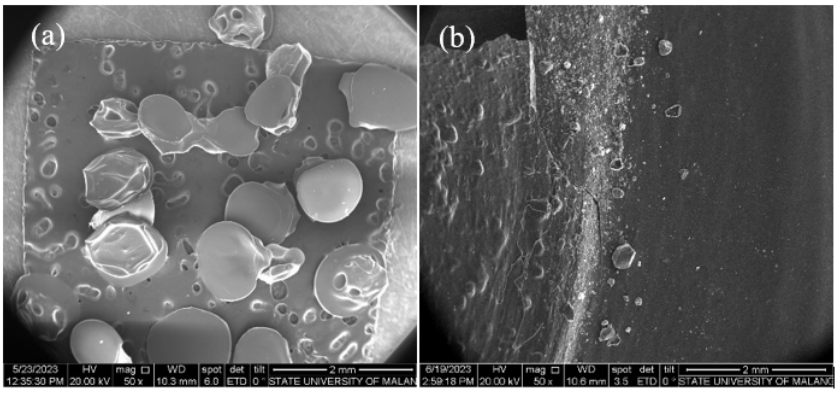

Fig. 5. Comparison of 50x magnification SEM morphology of (a) Ca-alginate and (b) Ca-alginate-silica

As shown in Fig. 5, Ca-alginate shows irregular particle morphology and is in the form of large and small spheres with a diameter of 138 nm. After the addition of silica, it shows that the difference in pore size fills the space on the pore surface so that the top layer has a non-smooth surface structure such as protruding particle stones.

3.6.2 Characterization of the Ca-Alginate-Carbon Membrane Using SEM

The morphology of the Ca-alginate with activated carbon membrane was analyzed using SEM. The characterization of the Ca-alginate-carbon membrane was performed at magnifications of 1500x and 5000x. The SEM of this membrane is shown in Fig. 6.

Morphological analysis of activated carbon to Ca-alginate membrane using 1500x and 5000x magnification was applied. The SEM image showed that the particles had a diameter of 347.89 nm. Ca-alginate membrane containing carbon has a particle diameter of 1 mm[14].

The resulting pore based on SEM results is a type of macropore. The analyzed pore size of Ca-alginate membrane without the addition of carbon was approximately 138 nm, exhibit a dense pore structure. A sparse pore structure would allow adsorbed substances to pass through, resulting in less effective outcomes. Crosslinking occurs between $CaCl_2$ and sodium alginate is more affective with addition of activated carbon.

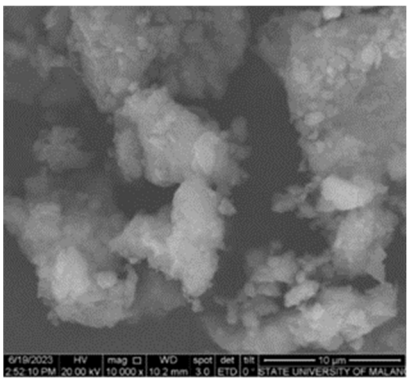

Fig. 6. SEM analysis of Ca-alginate-carbon membrane with 5000X magnification

3.7 Adsorption with variation of amount silica and carbon to Ca-alginate membrane

3.7.1 Optimization of Ca-Alginate-Silica Membrane Synthesis on the Sorption of Cl^- Ion

This optimization aims to find the optimal composition in the absorption of Cl^- ions. The adsorption process was carried out at a constant time of 40 minutes. As listed in Table 6, it is shown that the addition of silica with a mass of 0.05 grams produces the largest percentage of Cl^- ion adsorption. This is due to the increasing in silica mass is proportional to the amount number of active side to adsorb maximally Cl^- ion is shown in Fig.7.

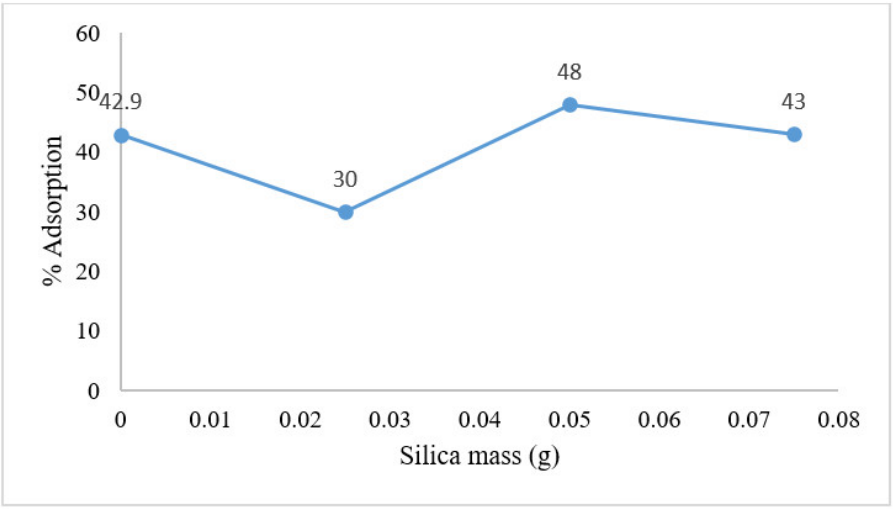

Fig. 7. Effect of silica mass in Ca-alginate-silica synthesis on Cl^- ion sorption

3.7.2 Optimization of Ca-Alginate-Carbon Membrane Synthesis on the Sorption of Cl^- Ion

Mass optimization of activated carbon was performed to determine the addition of carbon to get the most optimal adsorption capacity. The percentage adsorption of Na^+ and Cl^- ions is shown in Table 6. The effect of carbon mass in Ca-alginate-carbon synthesis is shown in Fig.8.

Table 6. Results of Adsorption of Na^+ and Cl^- Ions on Carbon Mass

Concentration (mg/L)			
Mass of Carbon (g)	**[Cl^-] initial**	**[Cl^-] adsorbed**	**% Adsorption**
-	3550	987.11	27.81
0.05	3550	1324.36	37.31
0.075	3550	1007.39	28.38
0.1	3550	826.27	23.28

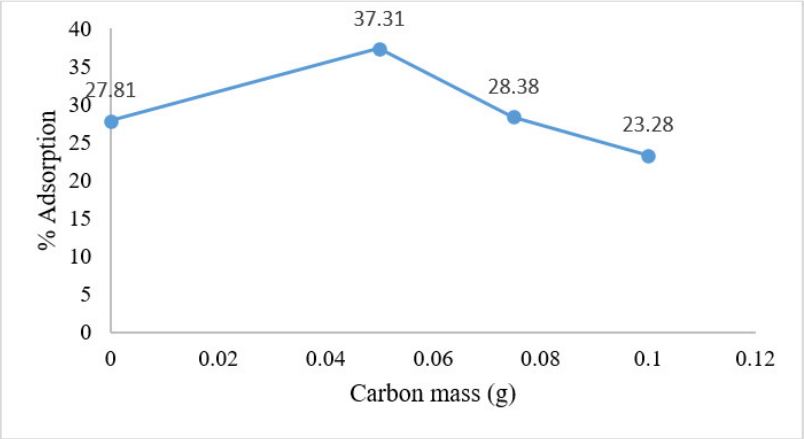

Fig. 8. Effect of carbon mass in Ca-alginate-carbon synthesis on Cl^- ion sorption

3.8 Application of Cl^- and Na^+ Ion Adsorption

3.8.1 Application of Ca-Alginate-Silica Membrane to Adsorption Cl^- and Na^+ with 0.1N NaCl

Table 7 shows that the contact time increases following the absorption of Cl^- ion. This shows that at the optimum condition of 40 minutes, reflecting an equilibrium and saturation point. This saturation point results in more interaction between the membrane and adsorbate, where Cl- ion is trapped in the membrane pores and bound by Ca^{2+} ions. The absorption of Cl^- ions decreased at 50 minutes and 60 minutes, which indicated the absorption of Cl^- ions desorbed or released back from the membrane.

The results of the Na^+ ion absorption test by Ca-alginate-silica produced an unstable adsorption percentage. As listed in Table 8, the maximum adsorption percentage was obtained at a contact time of 20 minutes by 55.4% Na^+ ion. This indicates that the optimum conditions due to the saturation point and interaction between the adsorbent and the adsorbed ions, indicating the Ca^{2+} ion in alginate is replaced by Na^+ ion bound to carboxyl groups (COO^-).

Table 7. Cl^- ion sorption with Ca-alginate-silica membrane

Concentration [Cl-] (mg/L)				
Contact time (minutes)	**Initial (real conc.)**	**Residual**	**Adsorbed**	**Adsorption Percentage (%)**
10	3536.492	2002.9	1533.5	43.4
20	3536.492	1878.8	1657.6	46.9
30	3536.492	1843.4	1693.09	47.9
40	3536.492	1790.2	1746.2	49.4
50	3536.492	1825.6	1710.8	48.4
60	3536.492	1878.8	1657.6	46.9

Conc. means concentration

Table 8. Na^+ ion sorption with Ca-alginate-silica membrane

Contact time (minutes)	**Concentration**			**Adsorption Percentage (%)**
	[Na^+] (mg/L)			
	Initial (real conc.)	**Residual**	**Adsorbed**	
10	1104.7	623.5	481.2	43.6
20	1104.7	492.7	612.01	55.4
30	1104.7	523.7	580.9	52.6
40	1104.7	766.5	338.2	30.6
50	1104.7	714.1	390.6	35.4
60	1104.7	537.05	567.6	51.4

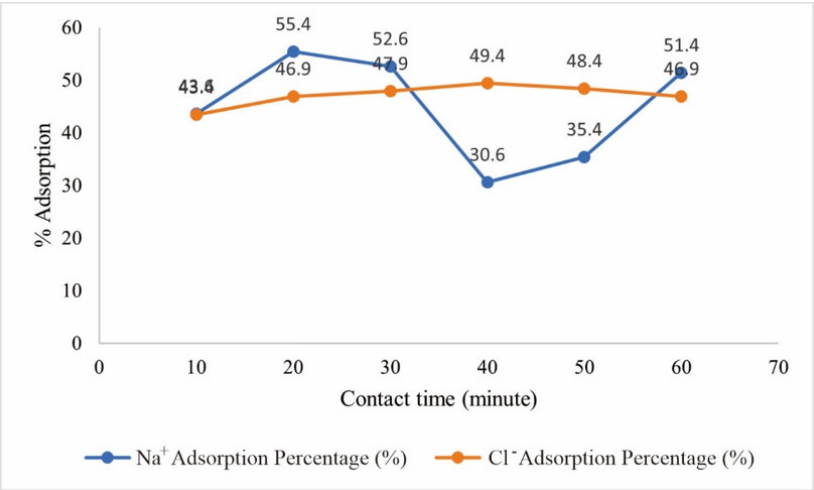

Fig. 9. Influence of contact time and percent adsorption of [Na^+] and Cl^- ions with Ca-alginate-silica membrane

As shown in Fig.9, the increase and decrease in the percent adsorption of Na^+ ion at each contact time is considered to be due to agglomeration (clot formation) in the membrane pores causing molecules to have limited access to the membrane surface. In addition, the absorption does not fluctuate due to the competitive cations in the absorption of Na^+ ion, especially K^+ cation terdetected in silica amounting to 0.43 gram/kg become competitor in Na^+ adsorption by Ca-alginate-silica.

3.8.2 Application of Ca-Alginate-C Membrane to Adsorption Cl^- and Na^+ ions

The use of Ca-alginate-C contact time is aimed to determine the optimum time for the membrane to absorb maximally of Na^+ and Cl^- ions. In this experiment, the contact times ranging from 5 to 35 minutes were used with 5-minute intervals. Adsorption of Na^+ and Cl^- ions was conducted using varying contact times to determine the optimal time during the adsorption process. The adsorption capacity concerning contact time is listed in Table 9.

Table 9. The adsorption of Na^+ and Cl^- ions by Ca-alginate-carbon

Contact Time (minutes)	Concentration (mg//L)		% Adsorption	Concentration (mg/L)		% Adsorption
	[Na^+] initial (real conc.)	[Na^+] adsorbed		[Cl^-] initial	[Cl^-] adsorbed	
5	1105.2	437.35	39.57	3550	971.1712	27.36
10	1105.2	478.7	43.31	3550	1188.518	33.48
15	1105.2	507.6	45.93	3550	1224.743	34.50
20	1105.2	542.1	49.05	3550	1260.967	35.52
25	1105.2	443.9	40.16	3550	1369.641	38.58
30	1105.2	400.5	36.24	3550	1659.437	46.74
35	1105.2	363.2	32.86	3550	1405.865	39.60

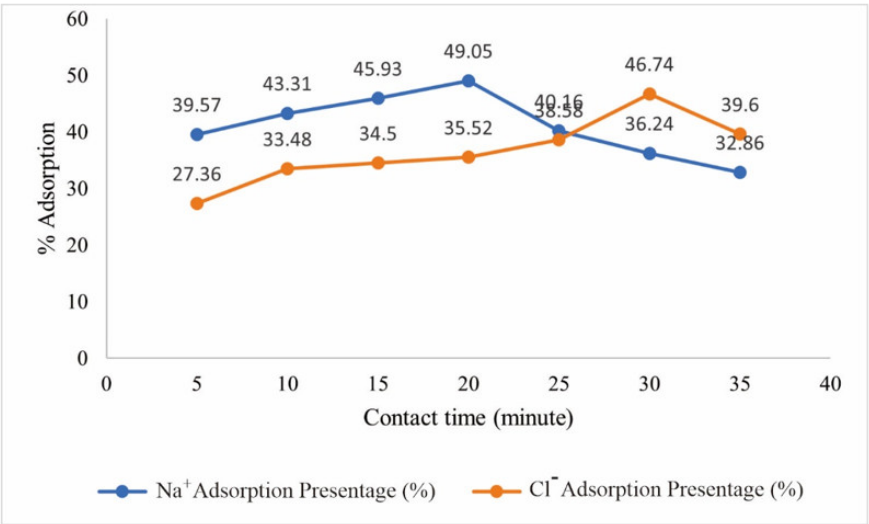

Fig. 10. The adsorption Na^+ and Cl^- ions on contact period by Ca-alginate-carbon

Ca-alginate-C membranes have carboxyl groups due to the addition of activated carbon which has carboxyl groups that provide additional functional groups, for increasing the absorbent of the membrane [15]. The range of contact time used for adsorption was 5 to 35 minutes with an interval of 5 minutes. The optimum time of activated carbon Ca-alginate membrane against Cl^- ion adsorption is at the 30th minute. From the 5 to 30th minute, there was an increase in adsorption power. At the 30th minute, the percent adsorption was obtained at 46%, while at the 35th minute the percent adsorption results decreased, which means that the membrane's ability to adsorb decreased. As shown in Fig.10, the adsorption of Na^+ ions increased in the 5 to 20th minute and reached the optimal adsorption value at a contact time of 20 minutes, then at the 25th time the adsorption of Na^+ ions decreased until the 35th

minute. The longer contact time given, the adsorption ability of the Ca-alginate-carbon membrane increased until a certain time limit after which it decreases, this is due to the membrane experiences saturation so that the adsorption ability decreases [16].

4 Conclusion

The optimized compositions of Ca-alginate-silica and Ca-alginate-carbon membranes reflected the distinct capacities for adsorbing Na^+ and Cl^- ions. In the optimized Ca-alginate-silica, 1% (w/v) alginate composition with 0.05 grams of silica revealed the remarkable adsorption rates: 55.4% for Na^+ ion within 20 minutes and 49.4% for Cl^- ion within 40 minutes. Conversely, the calcium alginate-carbon membranes, influenced by activated carbon, indicated the distinct shifts in functional group wavenumbers in FTIR analysis. The addition of activated carbon altered the spectra, revealing changes in hydroxyl (O-H) groups, C-H bonds, C=O bonds, and C-O groups. Moreover, the particle diameter notably increased from 138 nm to 347.89 nm in calcium alginate membranes with activated carbon. Optimal adsorption for calcium alginate-carbon membranes occurred with 0.05 grams of activated carbon, resulting in adsorption rates of 52.04% for Na^+ ions within 20 minutes and 37.31% for Cl^- ions within 30 minutes. These findings explained how the addition of activated carbon significantly impacted the membrane's functional groups and particle size, subsequently altering its adsorption capacities for Na^+ and Cl^- ions.

This research was funded by Penelitian Dasar Research on DRTPM 2023.

References

1. S. Honarparvar, X. Zhang, T. Chen, A. Alborzi, K. Afroz, & D. Reible, Frontiers of membrane desalination processes for brackish water treatment: A review. *Membranes*, **11** (2021). https://doi.org/10.3390/membranes11040246.
2. A. Armid, R. Shinjo, A. Takwir, R. Ruslan, & A. R. Wijaya, Spatial distribution and pollution assessment of trace elements Pb, Cu, Ni, Fe and as in the surficial water of Staring Bay, Indonesia. *Journal of the Brazilian Chemical Society*, **32** (2021) 299–310. https://doi.org/10.21577/0103-5053.20200180.
3. C. W. Suci, A. R. Wijaya, A. Santoso, & I. K. Kusumaningrum, Fe leaching in the sludge sediment of the prigi beach with tessier-microwave method. *AIP Conference Proceedings*, **2231** (2020). https://doi.org/10.1063/5.0002589.
4. A. R. Wijaya, F. Khoerunnisa, A. Armid, & R. A. Lusiana, The best-modified BCR and Tessier with microwave-assisted methods for leaching of Cu/Zn and their δ65Cu/δ66Zn for tracing sources in marine sediment fraction. *Environmental Technology and Innovation*, **28** (2022). https://doi.org/10.1016/j.eti.2022.102663.
5. M. Elma, N. Riskawati, & Marhamah, Silica Membranes for Wetland Saline Water Desalination: Performance and Long Term Stability. *IOP Conference Series: Earth and Environmental Science*, **175** (2018). https://doi.org/10.1088/1755-1315/175/1/012006.
6. A. R. Wijaya, I. K. Kusumaningrum, L. Hakim, A. Francová, V. Chrastný, M. Vítková, Z. Vaňková, & M. Komárek, Road-side dust from central Jakarta, Indonesia: Assessment of metal(loid) content, mineralogy, and bioaccessibility. *Environmental Technology and Innovation*, **28** (2022) 102934. https://doi.org/10.1016/j.eti.2022.102934.
7. A. R. Wijaya, F. Khoerunnisa, A. Armid, & R. A. Lusiana, The best-modified BCR and Tessier with microwave-assisted methods for leaching of Cu/Zn and their δ65Cu/δ66Zn

for tracing sources in marine sediment fraction. *Environmental Technology and Innovation*, **28** (2022) 102663. https://doi.org/10.1016/j.eti.2022.102663.

8. C. A. Schmidt, C. A. Stifler, E. L. Luffey, B. I. Fordyce, A. Ahmed, G. Barreiro Pujol, C. P. Breit, S. S. Davison, C. N. Klaus, I. J. Koehler, I. M. Lecloux, C. Matute Diaz, C. M. Nguyen, V. Quach, J. S. Sengkhammee, E. J. Walch, M. M. Xiong, E. Tambutté, S. Tambutté, T. Mass, & P. U. P. A. Gilbert, Faster Crystallization during Coral Skeleton Formation Correlates with Resilience to Ocean Acidification. *Journal of the American Chemical Society*, **144** (2022) 1332–1341. https://doi.org/10.1021/jacs.1c11434.
9. S. J. Randtke & C. P. Jepsen, Effects of Salts on Activated Carbon Adsorption of Fulvic Acids. *Journal / American Water Works Association*, **74** (1982) 84–93. https://doi.org/10.1002/j.1551-8833.1982.tb04854.x.
10. X. Zheng, K. Chen, & Z. Lin, Synthesis and Characterization of Alginate-Silica Gel Composites for Adsorption Dehumidification. *Industrial and Engineering Chemistry Research*, **59** (2020) 5760–5767. https://doi.org/10.1021/acs.iecr.9b06157.
11. A. L. Cazetta, A. M. M. Vargas, E. M. Nogami, M. H. Kunita, M. R. Guilherme, A. C. Martins, T. L. Silva, J. C. G. Moraes, & V. C. Almeida, NaOH-activated carbon of high surface area produced from coconut shell: Kinetics and equilibrium studies from the methylene blue adsorption. *Chemical Engineering Journal*, **174** (2011) 117–125. https://doi.org/10.1016/j.cej.2011.08.058.
12. A. R. Wijaya, S. Ohde, R. Shinjo, M. Ganmanee, & M. D. Cohen, *Geochemical fractions and modeling adsorption of heavy metals into contaminated river sediments in Japan and Thailand determined by sequential leaching technique using ICP-MS* (King Saud University, 2019). https://doi.org/10.1016/j.arabjc.2016.10.015.
13. S. Fatimah, Iswadi, & Muh. S. L, Sebagai Adsorben Air Sumur Yang Tercemar. **5** (2018) 109–118.
14. D. Q. Cao, K. Tang, W. Y. Zhang, C. Chang, J. L. Han, F. Tian, & X. Di Hao, Calcium Alginate Production through Forward Osmosis with Reverse Solute Diffusion and Mechanism Analysis. *Membranes*, **13** (2023) 1–15. https://doi.org/10.3390/membranes13020207.
15. H. G. Park, T. W. Kim, M. Y. Chae, & I. K. Yoo, Activated carbon-containing alginate adsorbent for the simultaneous removal of heavy metals and toxic organics. *Process Biochemistry*, **42** (2007) 1371–1377. https://doi.org/10.1016/j.procbio.2007.06.016.
16. A. P. Sedyanto, The Development of Fiber Adsorbent Based on Cassava Peel to Remove Pb Ion in Water. *Journal UII*, (2018) 1–17.